

# Friction between van der Waals Solids during Lattice Directed Sliding

Paul E. Sheehan<sup>\*,†,‡,§</sup> and Charles M. Lieber<sup>‡</sup>

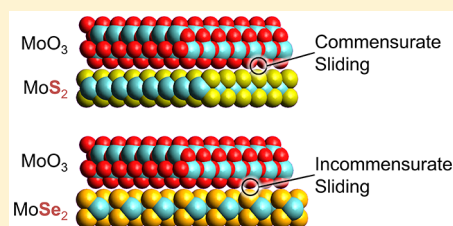
<sup>†</sup>U.S. Naval Research Laboratory, Code 6177, Washington, DC 20375, United States

<sup>‡</sup>Department of Chemistry and Chemical Biology, Harvard University, Cambridge, Massachusetts 02138, United States

**S** Supporting Information

**ABSTRACT:** Nanometer-scale crystals of the two-dimensional oxide molybdenum trioxide ( $\text{MoO}_3$ ) were formed atop the transition metal dichalcogenides  $\text{MoS}_2$  and  $\text{MoSe}_2$ . The  $\text{MoO}_3$  nanocrystals are partially commensurate with the dichalcogenide substrates, being aligned only along one of the substrate's crystallographic axes. These nanocrystals can be slid only along the aligned direction and maintain their alignment with the substrate during motion. Using an AFM probe to oscillate the nanocrystals, it was found that the lateral force required to move them increased linearly with nanocrystal area. The slope of this curve, the interfacial shear strength, was significantly lower than for macroscale systems. It also depended strongly on the duration and the velocity of sliding of the crystal, suggesting a thermal activation model for the system. Finally, it was found that lower commensuration between the nanocrystal and the substrate increased the interfacial shear, a trend opposite that predicted theoretically.

**KEYWORDS:** Tribology, transition metal dichalcogenides, 2D materials, shear stress, atomic force microscopy



Friction has been studied for centuries due to its clear industrial and technological importance. However, only in the last few decades have new tools arrived that can measure the fundamental atomic processes that govern friction and so test the many extant theories of friction.<sup>1–3</sup> Scanning probe microscopy (SPM) has been a particularly effective tool for tribology because it contacts the sample with a single, atomically sharp probe, a substantial simplification of the mechanics compared to most interfaces whose rough surfaces contact through multiple asperities, each bearing a different load.<sup>4</sup> Isolating the mechanics to a single contact has provided much needed insight into phenomena such as the effects of commensurability between the sliding surfaces,<sup>5</sup> tribomechanical reactions,<sup>6,7</sup> and the impact of velocity on friction.<sup>3</sup> It has also led to a shift in the analysis of friction with less emphasis on studying friction force versus load curves to extract friction coefficients and more emphasis on measuring the true contact area to extract the more fundamental interfacial shear strength, the force per unit area required to slide the sample.<sup>8–10</sup>

A separate yet related research thrust has been the assembly of nanoscale components into materials with properties inaccessible in their bulk counterparts. An example of this is the revived interest in van der Waals heterostructures<sup>11,12</sup> where two-dimensional solids with diverse physical and electronic properties such as graphene, boron nitride, and/or transition metal dichalcogenides are stacked to produce composite materials. While an initial consideration would suggest that these materials could be stacked arbitrarily, the chemical and physical coupling of the layers among themselves<sup>13</sup> and to the substrate<sup>13,14</sup> can be subtle and material dependent. Consequently, realizing the full potential of van der Waals heterostructures will require significant work to

understand the physical and chemical coupling between different layers.

One mechanical property found in van der Waals heterostructures but not in bulk materials is lattice directed sliding (LDS), where the motion of a nanocrystal of one 2D material is constrained to move along one of the crystallographic axes of a second 2D material on which it rests.<sup>15</sup> This constraint comes from a high degree of commensurability between the two materials along just one axis of the interface, which yields a single, low corrugation direction for easy sliding. LDS is most notably found in nanocrystals of  $\text{MoO}_3$  whose  $a$ -axes are rotated  $\sim 15^\circ$  with respect to the  $a$ -axes of the underlying  $\text{MoS}_2$  substrates (Figure 1). Both  $\text{MoO}_3$  and  $\text{MoS}_2$  are layered 2D materials with well-defined surface terminations. While moving along the easy sliding direction, the atoms of the 2D nanocrystal follow the grooves between the atoms of the stationary layer and so the two crystals remain aligned. This highly organized system is ideal for testing interlayer coupling while also resolving a significant challenge with SPM friction measurements: the apex of the scanning probe is occluded, hampering direct measurement of the contact area or the local stress distribution.<sup>4,8</sup> Moreover, the high forces involved make it difficult to maintain the crystallinity of the probe and to ensure that the tip and surface remain aligned during motion; although recent advances have shown that even probes with disordered contacts will respond to anisotropy on many substrates.<sup>5</sup>

**Received:** February 28, 2017

**Revised:** May 22, 2017

**Published:** June 1, 2017

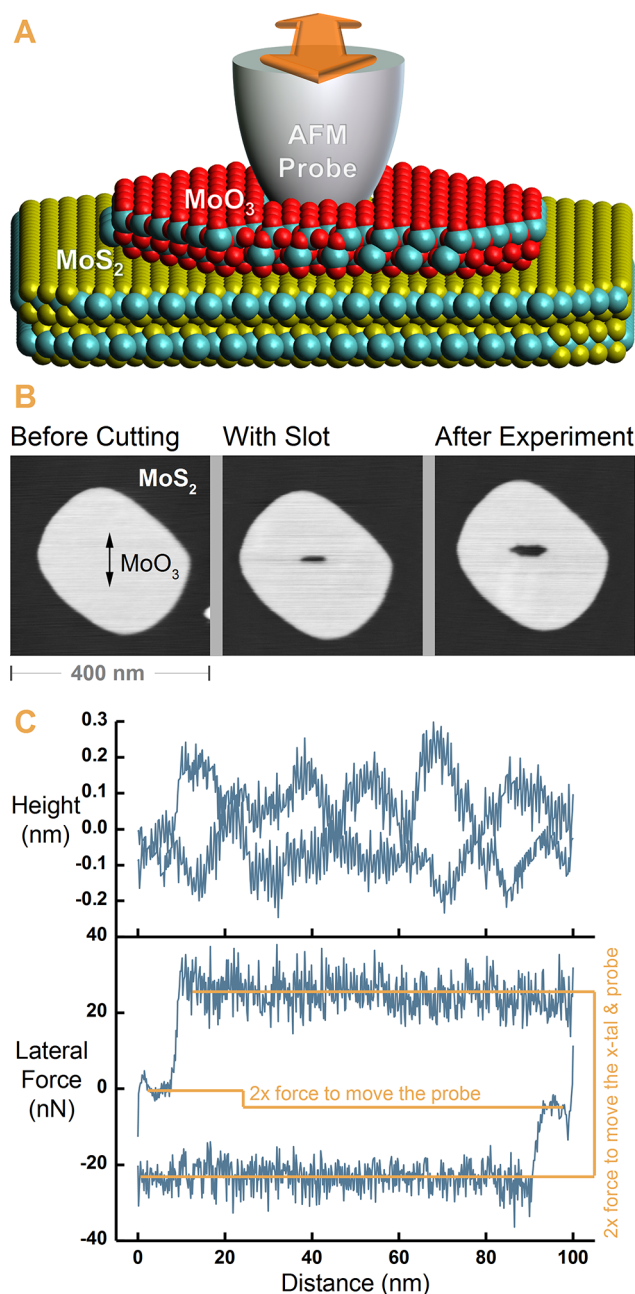


**Figure 1.** (A) The experimental configuration where the AFM probe has cut a thin slot in the MoO<sub>3</sub> nanocrystal which is then slid along the easy direction of the underlying lattice. (B) AFM images of a nanocrystals before machining, after machining the slot, and then after the experiment. Some wear at the edge of the slot was occasionally observed. (C) The upper plot shows that the probe remains in contact with the substrate during motion. The lower plot is a friction loop showing the lateral force on the probe as the nanocrystal was oscillated. The net force is half the height of the loop.

Here we describe studies of the sliding of MoO<sub>3</sub> nanocrystals on the surface of MoS<sub>2</sub> and MoSe<sub>2</sub> single crystals using an AFM probe both to move the nanocrystals and record lateral forces (Figure 1A, see Supporting Information for details). Studying the force required to move nanocrystals during LDS avoids questions of crystallinity and provides insight into several atomic-scale processes impacting friction. Because the contact area is well-defined, the interfacial shear may be confidently calculated, whereas examining different combinations of 2D

materials addresses the role of commensurability. Finally, experiments have provided extensive information on the role of velocity on friction, thereby inferring the contribution of interfacial heating to friction.

In our earlier experiments,<sup>15</sup> a small nanocrystal could be nudged short distances by the tip to provide an estimate of the shear strength; however, this approach could not probe velocity effects or follow the friction force over time. Our strategy to acquire more detailed information was to loosely affix the nanocrystal onto the tip. As noted above, the nanocrystal slides easily along one axis of the substrate but is held firmly perpendicular to this axis. This firm hold is sufficiently strong that a slot may be cut in a nanocrystal in the perpendicular direction by scanning the tip back and forth until the tip contacts the substrate (Figure 1B). After placing the tip in the formed slot, friction data would be acquired by oscillating the crystal in the easy sliding direction over a distance of 100 nm while monitoring the lateral force on the cantilever. The force on the probe as it moves to the end of the scan range and back is known as a friction loop (Figure 1c). Sliding in the forward direction causes positive deflection of the cantilever, whereas the return causes negative deflection. Averaging these two values removes instrumental offset and reduces the effect of noise.<sup>16</sup>

The initial regions of very low friction are due to the finite width of the slot which leaves a small gap between the tip and the edge of the nanocrystal where the tip slides on the substrate free of the MoO<sub>3</sub> crystal. While relatively small, typically less than 10% of the width of the friction loop, this force between the tip and substrate was routinely subtracted from the measured average. There are several advantages of this approach. It can continuously monitor friction as a function of time, velocity, and crystal size. It generates a substantial data set for analysis and circumvents the greatest unknown in scanning probe tribology experiments, the nature of the tip–substrate interface, because the entire crystal now acts as a stable, crystallographically aligned interface for the duration of the experiment.

Friction between the nanocrystal and the substrate should increase linearly with area.<sup>17</sup> Indeed, the proportionality constant between friction and area, the shear strength  $\tau$ , should be an intrinsic value for any interface. To measure the shear strength, the forces required to slide nanocrystals of different areas were measured as described above (Figure 2a). Examining the static (blue) data, it is clear that the required lateral force increases linearly with the nanocrystal area as expected, and the slope of the linear fit to the data yields a shear strength of  $0.44 \pm 0.04$  MPa.

This shear strength is quite small compared to those of the macroscopic system. Comprehensive friction studies of macroscopic MoS<sub>2</sub> thin films carried out in dry air by Singer et al. yielded a  $\tau = 24.8 \pm 0.5$  MPa,<sup>18</sup> a value 56 times larger than that found here for the preferred sliding direction of the MoO<sub>3</sub>/MoS<sub>2</sub> system. This suggests that the much larger average value of  $\tau$  found in macroscopic measurements arises in part from motion along high energy pathways and that if one could atomically align the sliding interface between macroscopic objects then friction should be dramatically reduced. Our microscopic value of  $\tau$  determined for MoO<sub>3</sub>/MoS<sub>2</sub>, 0.44 MPa, can also be compared to measurements of  $\tau$  for C<sub>60</sub> nanocrystals sliding on NaCl crystal surfaces<sup>19</sup> which at 0.1 MPa is a factor of 4 lower than our measurements of the MoO<sub>3</sub>/MoS<sub>2</sub> system. Part of this difference may reflect

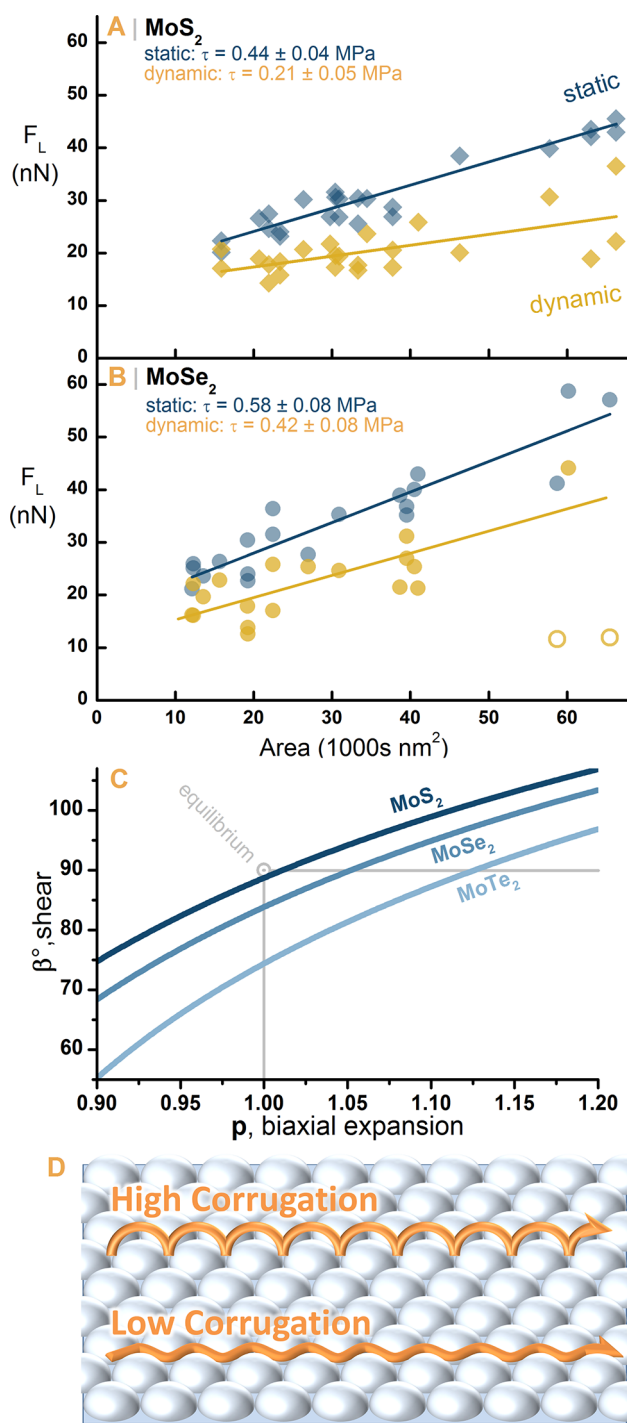


**Figure 2.** Lateral force required to slide the nanocrystals on MoS<sub>2</sub> (A) and MoSe<sub>2</sub> (B). The blue markers in both plots were taken from the first friction loop (static) while the yellow markers indicate the values in the dynamic steady state (yellow) after the presumed heating of the interface. The open dots were outliers and were not used in the fit. (C) Required shearing or expansion of MoO<sub>3</sub> for coincidence with various substrates. The intersection of a curve with the vertical gray line indicated the required pure shear for alignment, while intersection with the horizontal dashed line indicated the required biaxial expansion. A mixture of the two is possible. The gray circle indicates the equilibrium values of MoO<sub>3</sub>. (D) A schematic showing two possible pathways taken by the interfacial oxygen atoms as they traverse the substrate. Hopping over the atoms dissipates more energy than circumnavigating them.

differences in lattice commensurability and the molecular nature of the C<sub>60</sub> solid (which would reduce the true area of contact). Finally, Ritter et al. directly measured the shear strength of nanometer-scale, flake-like Sb nanocrystals on MoS<sub>2</sub> and found  $\tau \sim 115$  MPa. The much greater shear value reported in this work was attributed to the stresses induced by the relative motion of the petals of the nanocrystal which would enhance energy dissipation.

The linear fits in Figure 2 have nonzero y-axis intercepts, a result that was also observed when the shear stress was measured by other approaches (see Supporting Information for details). This result is interesting because most of the forces on the nanocrystal, such as shear, defects, and so forth, are proportional to the interfacial area, and so it suggests that the offset could measure the different friction behavior at the edges of the nanocrystal or perhaps local interaction with the tip. Measurements of smaller nanocrystals, which might distinguish these mechanisms, were not successful as we found them unlikely to maintain their integrity during motion. We also observed that large MoO<sub>3</sub> nanocrystals on MoSe<sub>2</sub> would occasionally have much lower shear strengths (see open circles in Figure 2B), which might be consistent with edge effects or contamination,<sup>20</sup> although additional studies in the future will be needed to fully address these points.

Experimental and theoretical work has shown that the commensurability of two surfaces impacts their friction.<sup>21–23</sup> Specifically, most theories predict a decrease in friction with increasing lattice mismatch and some predict that in the limit of an infinitely long incommensurate solid there will be an absence of friction, also called superlubricity.<sup>8,21,24</sup> To study this effect, we extended our measurements to MoO<sub>3</sub> nanocrystals undergoing lattice directed sliding on MoSe<sub>2</sub>. MoSe<sub>2</sub> has a larger lattice constant (3.29 Å) than MoS<sub>2</sub> (3.16 Å) and so should be less commensurate with the MoO<sub>3</sub> nanocrystal. This can be quickly seen if one makes the simplifying assumption that all the compliance to attain alignment occurs within the MoO<sub>3</sub> either through uniform biaxial expansion,  $p$ , or through shearing its lattice by an angle,  $\beta$ . Figure 2C plots these values for the molybdenum dichalcogenides with the gray dot showing the natural lattice angle, 90°, and  $p$  of the MoO<sub>3</sub>. The plot shows that MoO<sub>3</sub> would need only to expand or shear slightly to match the underlying MoS<sub>2</sub> lattice, whereas matching MoSe<sub>2</sub> requires much greater shear or expansion, indicating that the lattices are likely less aligned. Despite this lower commensurability, friction measurements on the MoO<sub>3</sub>/MoSe<sub>2</sub> system returned a shear stress,  $0.58 \pm 0.08$  MPa, which was 31% greater than that on MoS<sub>2</sub>.

The configuration of the MoO<sub>3</sub>/MoSe<sub>2</sub> interface that could lead to this increase in shear stress can be inferred from these experimental results and theoretical work.<sup>25,26</sup> First, that LDS was observed for MoO<sub>3</sub> on MoSe<sub>2</sub> strongly suggests alignment of the lattices. Second, the terminal oxygens of the MoO<sub>3</sub> nanocrystal, although stiff toward compression, have relatively soft bending modes and are thus relatively free to bend to seek out local minima.<sup>25</sup> Third, Diestler et al. found that the grooves in the substrate were the energetically favorable pathway for the oxygens to slide along.<sup>26</sup> Together, these suggest a model where the majority of the pendant oxygens reside in the substrate grooves thereby enabling LDS but that lattice mismatch will force some terminal oxygen atoms out of the grooves and into high corrugation pathways (Figure 2D). The greater dissipation from these high corrugation pathways leads to increased interfacial shear strength between the nanocrystal



and MoSe<sub>2</sub> substrate. This model is also consistent with our observation that MoO<sub>3</sub> nanocrystals rotate on MoSe<sub>2</sub> far more readily than on MoS<sub>2</sub>, suggesting a lower degree of commensuration.

Previous work has examined in detail the sliding of islands of different materials on MoS<sub>2</sub> or graphite when nudged by an AFM probe.<sup>15,19,20,27</sup> Here, loosely affixing the nanocrystal to the AFM probe enables for the first time tracking the change in friction with time. The probe was inserted into the slot and continuously oscillated 100 nm along the easy sliding axis at 2 Hz for 5 min while monitoring the friction force. Then, after a 5 min rest period the experiment would be repeated (Figure 3).

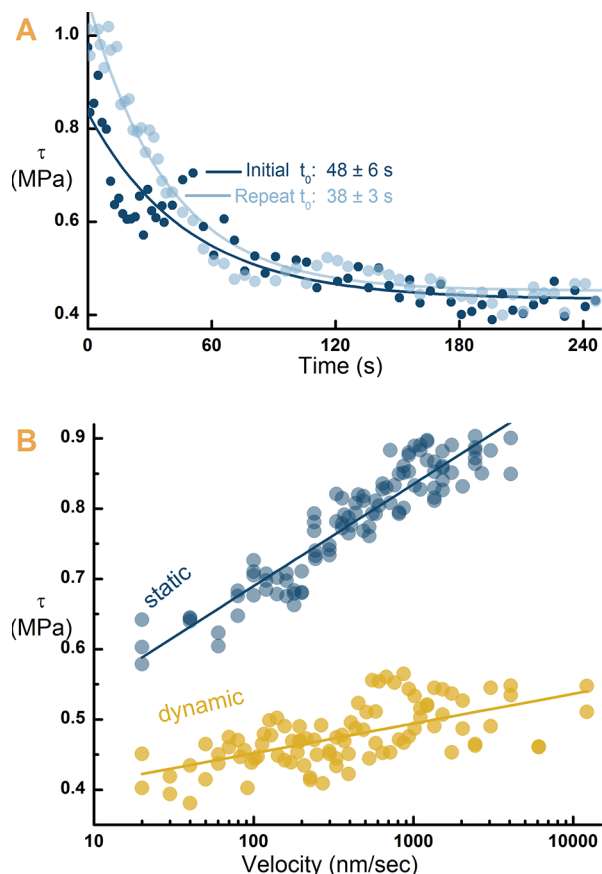


**Figure 3.** (A) The decay of interfacial shear with time. The two curves represent shear versus time data for the same (40 000 nm<sup>2</sup>) nanocrystal. The initial static data was acquired followed by a 5 min rest after which the repeat run was acquired. (B) Shear as a function of velocity. The interfacial shear of the nanocrystal was increased roughly logarithmically with velocity. The two data sets represent data acquired at intervals (static) and after continuous scanning to reach a steady state (dynamic). The data were acquired for both increasing decreasing velocity to check for instrumental drift or hysteresis. The fits are to eq 1 in the text.

For all the samples, the initial interfacial shear strengths were relatively high (Figure 3A) but then decreased quickly to a finite value that would be maintained indefinitely with continued sliding, whereas the plots above in Figure 2 show the initial friction force taken at the start of a run (static) and after continued sliding (dynamic) for several nanocrystals on both MoS<sub>2</sub> and MoSe<sub>2</sub>. To quantify the rate of decrease in friction force, the data were fit to an exponential to provide a decay constant,  $t_0$ , which varied only to a small degree among

the samples and did not correlate with either the nanocrystal dimensions or the substrate used. A histogram of these decay constants (Figure S4) indicates a mode of  $\sim 20$  s. After leaving the nanocrystal stationary for 5 min, the shear strength returned to the initial high value (Figure 3A), while repeating the oscillation sequence yielded a similar time-dependent drop in shear strength.

The reproducibility of the decrease with time indicates that the drop in friction was not due to a chemical reaction, an ordering of the interface, or other irreversible transformation but rather was inherent to the interface. Consequently, it does not appear to involve conventional static friction mechanisms. The most probable explanation for the drop in shear strength is thermolubricity, where heating the interface thermally activates the atom hopping needed for sliding.<sup>28,29</sup> Thermolubricity should be prominent in this system because both materials are lamellar with the lower out-of-plane thermal conductivity<sup>30</sup> enhancing the trapping of heat at the interface. This would especially enhance heating in the MoO<sub>3</sub>, which can only dissipate heat through the ambient or through the heated interface. A drop in friction with temperature was previously observed in Monte Carlo simulations that studied lattice directed sliding in the MoO<sub>3</sub>/MoS<sub>2</sub> system.<sup>26</sup> The final evidence for thermolubricity causing the temporal friction decay is that it also predicts the observed logarithmic increase in friction with sliding velocity as discussed below.

We have also studied the effect of velocity on shear strength using our experimental approach for scan velocities from 10 to 3600 nm/s. To increase the velocity, the scan range was held constant at 100 nm while the scan frequency was increased from 0.1 to 60 Hz. Because 60 Hz was the maximum frequency for this AFM, the scan range would be extended up to 1000 nm for the highest velocities. The results are shown in Figure 3B.

Since the shear strength varied with time, there were two constant regimes in which to take friction data: the initial static scan, presumably at room temperature, and the dynamic value where the temperature had reached a steady state. To probe the static regime, the nanocrystal was oscillated only once every 30 seconds in order to allow any generated heat to dissipate. We also limited the scan rate of the crystal to 10 Hz, because rates greater than this might generate excessive heat that could not be dissipated within those 30 s. Second, to probe the dynamic regime friction loops were acquired after oscillating the nanocrystal continuously for 5 min to equilibrate the interface. The results from a single nanocrystal are plotted in Figure 3 and reveal that the shear stress exhibits a strong logarithmic dependence in both regimes and that the slope for the static room temperature data is much steeper than for the dynamic data.

The variation of friction with velocity can depend on several factors including cleanliness, the presence of a liquid meniscus,<sup>31</sup> and the potential for chemical rebonding.<sup>8,32</sup> These latter two effects cause a logarithmic decrease in friction with increased velocity, which, although not observed, could alter the values extracted by the fit if present. However, chemical rebonding is unlikely because both the nanocrystals and the substrates are 2D materials with fully satisfied bonds that also cannot participate in the hydrogen bonding associated with this mechanism. Second, while meniscus formation can decrease friction in hydrophilic systems, both MoS<sub>2</sub> and MoSe<sub>2</sub> are relatively hydrophobic. This mechanism also requires the formation of a layer of water between the nanocrystal slider and substrate, which appears incompatible with the observed

maintenance of LDS. Finally, the friction decrease due to a meniscus is typically observed at atmospheric levels of humidity because it scales as  $\propto -[\ln(\text{relative humidity})]^{-1}$  and so is unlikely to impact friction in the xeric conditions of the glovebox ( $\text{H}_2\text{O} < 0.1$  ppm).<sup>33</sup>

Riedo et al. showed that for small, well-defined contacts in the absence of these effects the friction force should increase logarithmically with the velocity.<sup>3,34</sup> This model builds on the Prandtl–Tomlinson model that views the system as a moving mass that interacts with the corrugated substrate via pendant springs terminated by pointlike tips. Dissipation occurs via these springs, and the moving mass is considered rigid. Geometrically, the  $\text{MoO}_3$  nanocrystals with their pendant oxygens seem to fit this description closely. In the thermal Prandtl–Tomlinson model, friction plateaus at high velocities, a behavior not observed in these experiments. This enables us to use the low velocity relationship developed by Gyalog et al.<sup>1</sup>

$$F(v) = F_{\max} - \left[ \beta k_B T \ln \left( \frac{v_0}{v} \right) \right]^{2/3} \quad (1)$$

where  $\beta$  relates the energy barrier jumped to the applied lateral force  $\Delta E = (1/\beta)(F_{\max} - F_x)^{3/2}$  and  $v_0$  is a critical velocity

$$v_0 = \frac{2f_0 \beta k_B T}{3c_x \sqrt{F_{\max}}} \quad (2)$$

Figure 3B shows the data fit to this model. At room temperature, the model fit reasonably well ( $R^2 = 0.86$ ), giving a  $F_{\max} = 53.04 \pm 7.61$  nN, a  $\beta = 0.93 \pm 0.19$   $\text{nN}^{3/2}/k_B T$ , and a  $v_0 = 128 \pm 455$   $\mu\text{m/s}$ . The large error in the value of  $v_0$  is expected because the data did not show the plateau behavior that should appear when  $v_0$  is reached. Although the data in the dynamic regime could also be fit ( $F_{\max} = 27.26 \pm 1.10$  nN,  $\beta = 0.51 \pm 0.11$   $\text{nN}^{3/2}/k_B T$ ,  $v_0 = 12 \pm 22$   $\mu\text{m/s}$ ), greater caution is warranted. Specifically, because the power dissipated scales linearly with velocity and the temperature should rise with dissipated power, these data were effectively collected over a range of temperatures. This may also explain the lower coefficient of determination ( $R^2 = 0.40$ ). Future work with systems that can independently control the temperature of the sample would provide greater insight.

In conclusion, tribological experiments revealed the rich mechanical coupling between 2D materials and because of the much greater level of system definition provided additional insight into friction at the atomic scale. Lattice directed sliding was observed for  $\text{MoO}_3$  on both  $\text{MoS}_2$  and  $\text{MoSe}_2$ , even though the latter was less commensurate with the  $\text{MoO}_3$ . LDS also led to measured shear values that were far lower than for macroscale contacts. On  $\text{MoSe}_2$ , the nanocrystals had a greater interfacial shear strength even though they were less commensurate, a trend opposite to theory and prior experiment but which may be explained by a subpopulation of the interfacial atoms being dragged along high energy pathways. Finally, a thermal activation model explains much of the behavior in the system with higher shear values at higher velocities and the reproducible drop in friction with time.

## ■ ASSOCIATED CONTENT

### Supporting Information

The Supporting Information is available free of charge on the ACS Publications website at DOI: 10.1021/acs.nanolett.7b00871.

Detailed methods and additional figures describing the growth  $\text{MoSe}_2$  single crystals, growth and selection of  $\text{MoO}_3$  nanocrystals, and measurement and analysis of shear stress (PDF)

## ■ AUTHOR INFORMATION

### Corresponding Author

\*E-mail: paul.sheehan@nrl.navy.mil.

### ORCID

Paul E. Sheehan: 0000-0003-2668-4124

### Notes

The authors declare no competing financial interest.

## ■ ACKNOWLEDGMENTS

P.E.S. thanks Dr. K. Wahl for a careful reading of the manuscript. P.E.S. acknowledges support at the U.S. Naval Research Laboratory from the Nanoscience Institute. C.M.L. acknowledges support of work at Harvard University from the Air Force Office of Scientific Research.

## ■ REFERENCES

- (1) Gnecco, E.; Meyer, E. *Fundamentals of Friction and Wear*; Springer: Berlin, 2007.
- (2) Persson, B. N. J. *Sliding Friction Physical Principles and Applications*; Springer: Berlin, 2000.
- (3) Riedo, E.; Gnecco, E.; Bennewitz, R.; Meyer, E.; Brune, H. *Phys. Rev. Lett.* **2003**, *91*, 084502.
- (4) Carpick, R. W.; Salmeron, M. *Chem. Rev.* **1997**, *97*, 1163–1194.
- (5) Balakrishna, S. G.; de Wijn, A. S.; Bennewitz, R. *Phys. Rev. B: Condens. Matter Mater. Phys.* **2014**, *89*, 89.
- (6) Gosvami, N. N.; Bares, J. A.; Mangolini, F.; Konicek, A. R.; Yablon, D. G.; Carpick, R. W. *Science* **2015**, *348*, 102–106.
- (7) Felts, J. R.; Oyer, A. J.; Hernandez, S. C.; Whitener, K. E.; Robinson, J. T.; Walton, S. G.; Sheehan, P. E. *Nat. Commun.* **2015**, *6*, 6467.
- (8) Park, J. Y.; Salmeron, M. *Chem. Rev.* **2014**, *114*, 677–711.
- (9) Carpick, R. W.; Ogletree, D. F.; Salmeron, M. *Appl. Phys. Lett.* **1997**, *70*, 1548–1550.
- (10) Lantz, M. A.; O'Shea, S. J.; Welland, M. E.; Johnson, K. L. *Phys. Rev. B: Condens. Matter Mater. Phys.* **1997**, *55*, 10776–10785.
- (11) Geim, A. K.; Grigorieva, I. V. *Nature* **2013**, *499*, 419–425.
- (12) Koma, A. *Thin Solid Films* **1992**, *216*, 72–76.
- (13) Andersen, K.; Latini, S.; Thygesen, K. S. *Nano Lett.* **2015**, *15*, 4616–4621.
- (14) Tsoi, S.; Dev, P.; Friedman, A. L.; Stine, R.; Robinson, J. T.; Reinecke, T. L.; Sheehan, P. E. *ACS Nano* **2014**, *8*, 12410–12417.
- (15) Sheehan, P. E.; Lieber, C. M. *Science* **1996**, *272*, 1158–1161.
- (16) Bhushan, B. *Handbook of micro/nanotribology*; CRC Press: Boca Raton, 1995; pp 44–50.
- (17) Bowden, F. P.; Tabor, D. *The Friction and Lubrication of Solids*. Oxford University Press: New York, 1950; pp 111–113.
- (18) Singer, I. L.; Bolster, R. N.; Wegand, J.; Fayeulle, S.; Stupp, B. C. *Appl. Phys. Lett.* **1990**, *57*, 995–997.
- (19) Luthi, R.; Meyer, E.; Haefke, H.; Howald, L.; Gutmannsbauer, W.; Guntherodt, H. J. *Science* **1994**, *266*, 1979–1981.
- (20) Dietzel, D.; Ritter, C.; Monninghoff, T.; Fuchs, H.; Schirmeisen, A.; Schwarz, U. D. *Phys. Rev. Lett.* **2008**, *101*, 125505.
- (21) van Wijk, M. M.; Dienwiebel, M.; Frenken, J. W. M.; Fasolino, A. *Phys. Rev. B: Condens. Matter Mater. Phys.* **2013**, *88*, 88.
- (22) Muser, M. H.; Wenning, L.; Robbins, M. O. *Phys. Rev. Lett.* **2001**, *86*, 1295–1298.
- (23) Dienwiebel, M.; Verhoeven, G. S.; Pradeep, N.; Frenken, J. W.; Heimberg, J. A.; Zandbergen, H. W. *Phys. Rev. Lett.* **2004**, *92*, 126101.
- (24) Berman, D.; Deshmukh, S. A.; Sankaranarayanan, S. K.; Erdemir, A.; Sumant, A. V. *Science* **2015**, *348*, 1118–22.
- (25) Py, M. A.; Maschke, K. *Physica B+C* **1981**, *105*, 370–374.

- (26) Diestler, D. J.; Rajasekaran, E.; Zeng, X. C. *J. Phys. Chem. B* **1997**, *101*, 4992–4997.
- (27) Ritter, C.; Baykara, M. Z.; Stegemann, B.; Heyde, M.; Rademann, K.; Schroers, J.; Schwarz, U. D. *Phys. Rev. B: Condens. Matter Mater. Phys.* **2013**, *88*, 045422.
- (28) Krylov, S. Y.; Jinesh, K. B.; Valk, H.; Dienwiebel, M.; Frenken, J. W. *Phys. Rev. E Stat. Nonlin. Soft Matter Phys.* **2005**, *71*, 065101.
- (29) Jansen, L.; Holscher, H.; Fuchs, H.; Schirmeisen, A. *Phys. Rev. Lett.* **2010**, *104*, 256101.
- (30) Liu, J.; Choi, G. M.; Cahill, D. G. *J. Appl. Phys.* **2014**, *116*, 233107.
- (31) Liu, H. W.; Ahmed, S. I. U.; Scherge, M. *Thin Solid Films* **2001**, *381*, 135–142.
- (32) Chen, J.; Ratera, I.; Park, J. Y.; Salmeron, M. *Phys. Rev. Lett.* **2006**, *96*, 236102.
- (33) Riedo, E.; Levy, F.; Brune, H. *Phys. Rev. Lett.* **2002**, *88*, 185505.
- (34) Muser, M. H. *Phys. Rev. Lett.* **2002**, *89*, 224301.